Proceedings of 8th International Stirling Engine Conference, p. 19-28, 1997

PERFORMANCE EVALUATION FOR A 100 W STIRLING ENGINE

Koichi HIRATA[*1], Shoichi IWAMOTO[*1], Fujio TODA[*1] and Kazuhiro HAMAGUCHI[*2]

[*1]Department of Mechanical Engineering, Faculty of Engineering, Saitama University, Japan
[*2]Hokkaido Polytechnic College, Japan

ABSTRACT

A small 100 W displacer-type Stirling engine, Ecoboy-SCM81 has being developed by a committee of the Japan Society of Mechanical Engineers. The engine contains unique features, including an expansion cylinder which is heated by either combustion gas or direct solar energy. Also, a simple cooling system rejects heat from the working gas. A displacer piston has both heating and cooling inner tubes for the working gas which flows to and from outer tubes. A regenerator is located in the displacer piston.

To improve the engine performance efficiently, an analysis model for the prototype engine was developed. The analysis model is based an isothermal method considered a pressure loss in the regenerator, a buffer space loss caused by a leakage of the working gas, and a mechanical loss. In the case of a calculation for the pressure loss, the analysis model adopts a new suggestion that considers effects of entrance and exit area on the velocity distribution in the regenerator. The buffer loss is calculated with three kinds of methods, an isothermal, an adiabatic and a heat transfer model to consider a suitable method for the buffer space model. Some improvement methods for the prototype engine are discussed after the effectiveness of the analysis model is evaluated.

INTRODUCTION

From 1994 to 1996, a committee called RC127, was organized in the Japan Society of Mechanical Engineers. One of the projects of RC127 developed a small 100 W displacer-type Stirling engine[1)]. The goal of the engine performance was an output of 100 W with 20 % thermal efficiency. The engine was constructed based on detailed blueprints and was named Ecoboy-SCM81. From the initial experimental result, it became clear that the prototype engine has a maximum output power of 74 W at 0.8 MPa mean engine pressure operating at 1300 rpm engine speed[2)]. In order to collect adequate information for design methods, an evaluation of the engine performance and analysis methods of the experimental results of the engine have been discussed.

In this paper, one of the considered analysis models for the prototype engine is presented. The analysis model is based on an isothermal method considered some thermal losses, and have been developed to discuss the improvements for the engine performance. The engine performance was also measured by using nitrogen or helium as the working gas to evaluate the effectiveness of the analysis model.

ANALYSIS MODEL

Figure 1 shows the prototype engine. Table 1 shows its specifications and target performance. It is difficult to analyze temperatures in the working space in detail, because the heat exchangers have particular features. Then, in the analysis model, the engine pressure is calculated by an isothermal model. And this model can treat several losses: a pressure loss in the regenerator, gas leakage from working spaces to a buffer space, a buffer space loss and a mechanical loss. The analysis methods of these heat losses are mentioned in this chapter.

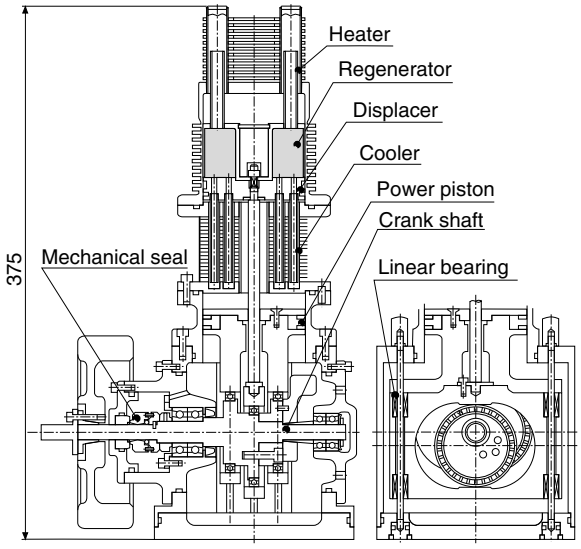

Figure 1 SCHMATIC VIEW OF ECOBOY-SCM81

Table 1 SPECIFICATIONS AND TARGET ERFORMANCE

Engine type	Displacer type (gamma configuration)
Working gas	Helium/Air
Mean engine pressure	~ 1 Mpa
Expansion space temp.	~ 923 K
Compression space temp.	~ 343 K (Water/Air cooling)
Engine speed	1000 rpm
Bore x Stroke	72 x 20mm
Output power	100 W
Thermal efficiency	20 %

CALCULATION OF PRESSURE

Figure 2 shows the analysis model. The working space is divided into five spaces, an expansion space, a regenerator space, a compression space, a pass space, and a piston space as shown in this figure. To analyze the engine performance theoretically, an isothermal model which can use the temperatures based on the experimental result, is adopted. When there is an assumption that each spaces maintain isothermal during the cycle without any thermal losses, the engine pressure, P, is calculated by Eq. 1 from the overall mass in the working space, m_{eng}, a gas constant, R, each volumes, V and each gas temperatures, T.

$$P = \frac{m_{eng} R}{\frac{V_E}{T_E} + \frac{V_R}{T_R} + \frac{V_C}{T_C} + \frac{V_{CP}}{T_{CP}} + \frac{V_P}{T_P}} \quad (1)$$

PRESSURE LOSS

Stirling engines have pressure losses at heater, regenerator, cooler and their connection parts. In the case of the prototype engine, major pressure loss generates in the regenerator, because the heater and cooler consist of short tubes and have enough extent of section area for the working gas flow. This analysis model considers only the pressure loss in the

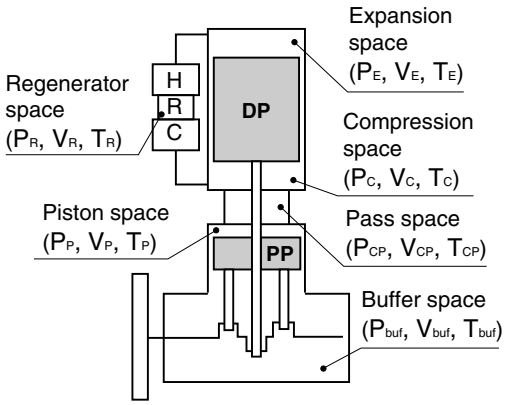

Figure 2 ANALYSIS MODEL

regenerator. In the case of the prototype engine, it is difficult to estimate the pressure loss by using generally proposed equations for stacked mesh. Because Spring Mesh, which is a porous type matrix consisting of pressed zigzag stainless steel wires is used as the matrix[2),3)]. Then, an estimated method which is defined from a porosity of the matrix and a hydraulic diameter, is used for the calculation.

The hydraulic diameter, h_{dy} is calculated as shown in Eq. 2 using the porosity, ε and a wire diameter, d.

$$d_{hy} = \frac{\varepsilon d}{1-\varepsilon} \tag{2}$$

A pressure drop at both ends of the regenerator, ΔP is calculated as shown in Eq. 3 using a friction factor, f_R, a length of the regenerator, H_R, a density of the working gas, ρ_R and a velocity of the working gas in the regenerator, u_R.

$$\Delta P = f_R \frac{H_R}{d_{hy}} \frac{\rho_R u_R{}^2}{2} \tag{3}$$

The friction factor, f_R is calculated as shown in Eq. 4 proposed by Tanaka[4)] using Reynolds number, Re.

$$f_R = \frac{175}{Re} + 1.60 \tag{4}$$

The velocity, u_R is calculated as shown in Eq. 5 using a gas mass flow in the regenerator, Q_R per porosity, ε, a section area of the regenerator housing, A and the density, ρ_R.

$$u_R = \frac{Q_R}{\varepsilon A \rho_R} \tag{5}$$

Reynolds number, Re is calculated as shown in Eq. 6 using a viscosity of the working gas, μ.

$$Re = \frac{d_{hy} u_R \rho_R}{\mu} \tag{6}$$

The pressure losses of many kinds of the regenerators including Spring Mesh can be estimated by above equations.

Next, effect of entrance and exit area on the velocity distribution in the regenerator is considered[5),6)]. A section ratio, m, is defined as the section area of the regenerator housing, A, by that of regenerator end, B. A distance, x (mm) is defined as a length of flow direction from the end. A section area, S is considered with the effect of entrance and exit area on the velocity distribution in the regenerator. A flow section area ratio, S/A at the distance, x, can be calculated as shown in Eq. 7.

$$\frac{S}{A} = 1 - (1-m) \cdot \exp(-0.367 \cdot mx) \tag{7}$$

Table 2 shows specifications of heat

Table 2 SPECIFICATION OF HEAT EXCHANGER SYSTEM

	Heater	Cooler
Type	Double tube	Double tube
No. tubes	10	24
Diameters of tubes (OD, ID) (mm)		
inner	9.5, 7.0	5.0, 4.0
outer	13.8, 12.4	8.0, 7.4
Length of tubes (mm)	54	56
Material	Stainless steel	Copper

	Regenerator
Type	Annular tube
Unit No.	1
Diameters (mm)	
inner	27
outer	66
Length of tubes (mm)	35
Matrix material	Stainless steel

exchanger system of the prototype engine. In the case of the prototype engine, the section ratio, m at the heater side is led to 0.135, and that of the cooler side is led to 0.106. The section area ratio, S/A is calculated by Eq. 7 as shown in Fig. 3. This figure shows that the working gas flows without an enough extending in the regenerator.

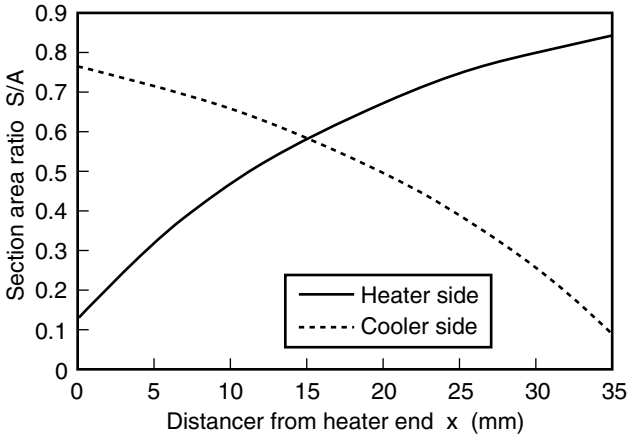

Figure 3 SECTION AREA RATIO

Then, the analysis model is needed to correct the velocity of the working gas with the consideration of the section area ratio, S/A. But it is difficult to analyze the flow pattern in detail with the effects of both the heater and cooler side. A value of the section area ratio, S/A to 0.55 is used following calculations. This value is an average of that of the heater and cooler side.

The total pressure loss, L_{ploss} considered with the effect of the entrance and exit area on the velocity distribution in the regenerator can be defined as shown in Eq. 8 using the pressure drop, P and the engine speed, n (rps).

$$L_{ploss} = \circ \; P \times dV_E \times n \tag{8}$$

LEAKAGE OF WORKING GAS

The gas leakage between the working space and the buffer space is supposed as an adiabatic flow in a Laval nozzle[7]. The gas leakage flow rate, dm/dt is calculated as shown in Eq. 9 and Eq. 10 using a specific heat ratio, , a higher pressure, P_{high}, a lower pressure, P_{low}, a gas temperature at upper flow side, T_{in}, and an equivalent diameter of the nozzle, d_{leak}.

$$\text{When, } \frac{P_{high}}{P_{low}} \quad \frac{2}{+1}\div^{\overline{\ 1}}; \quad \frac{dm}{dt} = \frac{d_{leak}^{\ 2}}{4}\sqrt{\frac{2}{+1}\div^{\overline{\ 1}}\times\frac{P_{high}^{\ 2}}{RT_{in}}} \tag{9}$$

$$\text{When, } \frac{P_{high}}{P_{low}} > \frac{2}{+1}\div^{\overline{\ 1}}; \quad \frac{dm}{dt} = \frac{d_{leak}^{\ 2}}{4}\sqrt{\frac{2}{1}\times\frac{P_{high}^{\ 2}}{RT_{in}}\ \frac{P_{high}}{P_{low}}\div^{\overline{\ 2}}\ \ \frac{P_{high}}{P_{low}}\div^{\overline{\ +1}}} \tag{10}$$

In the following calculations, the equivalent diameter, d_{leak}, is equaled 0.95 mm. This value was derived from an experimental result with the prototype engine.

BUFFER SPACE LOSS

It is difficult to analyze thermal characteristics of the working gas in the buffer space. Because there are some mechanical parts which heat themselves in the buffer space. Then three different calculated models were used for the buffer space in this analysis model.

(1) Isothermal model

The buffer space pressure, P_{buf} is calculated by Eq. 11 from the mass of the buffer space, m_{buf} and the buffer volume, V_{buf} under an assumption that the buffer space maintains the gas

temperature, T_{buf} during the cycle.

$$P_{buf} = \frac{m_{buf} R T_{buf}}{V_{buf}} \tag{11}$$

(2) Adiabatic model

When there is an assumption that the buffer space gas changes adiabatically, the energy equation is shown in Eq. 12 using a specific heat at constant volume, c_v, a specific heat at constant pressure, c_p and the gas temperature of the upper flow space, T_{in}.

$$c_v \frac{d(m_{buf} T_{buf})}{dt} = c_p \frac{dm}{dt} T_{in} - P_{buf} \frac{dV_{buf}}{dt} \tag{12}$$

Equation 12 is changed in Eq. 13, using a crank angle, θ.

$$\frac{dT_{buf}}{d\theta} = \frac{\kappa}{m_{buf}} \frac{dm}{d\theta} T_{in} - (\kappa - 1) \frac{T_{buf}}{V_{buf}} \frac{dV_{buf}}{d\theta} \tag{13}$$

The buffer space temperature, T_{buf} can be calculated by solutions of above differential equation. Then the buffer space pressure, P_{buf} is calculated by Eq. 11.

(3) Heat transfer model

In the case with consideration that the working gas in the buffer space is affected by heat transfers from the buffer space wall and the mechanical parts, an energy equation is shown in Eq. 14, using a heat transfer coefficient, h, a heat transfer area, A_{buf} and a buffer space wall temperature, T_{wbuf}.

$$c_v \frac{d(m_{buf} T_{buf})}{dt} = c_p \frac{dm}{dt} - P_{buf} \frac{dV_{buf}}{dt} + hA_{buf} (T_{wbuff} - T_{buf}) \tag{14}$$

Equation 14 is changed in Eq. 15, using a number of heat transfer unit, N_{tu} defined by Eq. 16.

$$\frac{dT_{buf}}{d\theta} = \frac{\kappa}{m_{buf}} \frac{dm}{d\theta} T_{in} - (\kappa - 1) \frac{T_{buf}}{V_{buf}} \frac{dV_{buf}}{d\theta} + \kappa \cdot N_{tu} (T_{wbuff} - T_{buf}) \tag{15}$$

$$N_{tu} = \frac{hA_{buf}}{2\pi n c_p m_{buf}} \tag{16}$$

When the number of heat transfer unit, N_{tu} is set adequately, the buffer space temperature, T_{buf} and pressure, P_{buf} can be calculated by solutions of above differential equation.

INDICATED WORK AND POWER

An expansion power, L_E, a compression power, L_C and a piston space power, L_P are calculated as shown in next equations, using each pressures and volumes.

$$L_E = \oint P_E dV_E \cdot n \tag{17}$$

$$L_C = -\oint P_C dV_C \cdot n \tag{18}$$

$$L_P = \oint P_P dV_P \cdot n \tag{19}$$

A buffer space loss, L_{buf} is calculated as shown in Eq. 20.

$$L_{buf} = -\oint P_{buf} dV_{buf} \cdot n \tag{20}$$

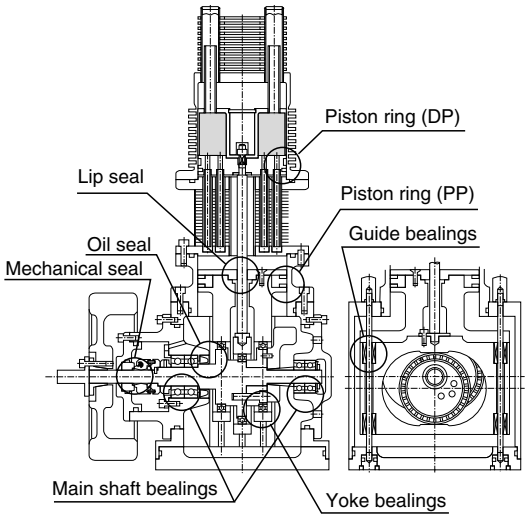

Figure 4 FACTOR OF MECHANICAL LOSS

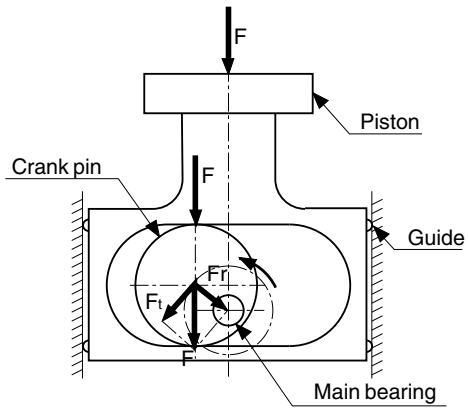

Figure 5 CALCULATION MODEL OF MECHANICAL FORCE

An indicated power, L_i, considered the buffer space loss is calculated as shown in Eq. 21.

$$L_i = L_E \quad L_C + L_P \quad L_{buf} \tag{21}$$

MECHANICAL LOSS

Figure 4 shows factors of the mechanical loss of the prototype engine. The mechanical loss consists of a coulomb friction loss and a viscosity friction loss. The coulomb friction loss is affected by mechanical forces only. The viscosity friction loss is affected by lubricating devices mainly.

Figure 5 shows a calculation model of the mechanical forces[1),8)]. The coulomb friction loss is calculated to be based the mechanical forces.

In the case of the prototype engine, lubricating oil for the mechanical seal and grease in the bearings cause the viscosity friction loss. It is difficult to calculate these losses analytically. Because the losses are affected from operating conditions like temperatures. In this analysis model, the viscosity friction loss is led by an approximate equation based experimental results.

COMPARISON TO EXPERIMENTAL RESULTS

EXPERIMENTAL AND CALCULATED CONDITIONS

Table 3 shows experimental conditions. A 1 kW (max.) electric heater was used to heat the engine. Heat input from the electric heater was adjusted to maintain the expansion space gas temperature to 703 K.

On the other hand, the temperatures for following calculations are set the expansion gas temperature, T_E to 703 K, the

Table 3 EXPERIMENTAL CONDITIONS

Heat source	Electric heater
Expansion gas temp.	703 K
Working gas	He / N_2
Mean engine pressure	0.8 MPa
Regenerator	Spring Mesh
Cooling type	Water cooling
Piston ring	4-piece type

compression gas temperature, T_C to 323 K, the piston space gas temperature, T_P to 303 K and the buffer space mean gas temperature, T_{buf} to 313 K based the results of the experiments. The regenerator gas temperature, T_R is set to the value of average between T_E and T_C. The pass space gas temperature, T_{CP} is set to the average between T_C and T_P.

PRESSURE LOSS

Figure 6 shows the relation between the engine speed and the pressure loss for both the calculation and the experiment. This figure shows that the difference of working gas are expressed well, though the calculated result was slightly higher than the experimental results.

The section area ratio, S/A was set to 0.55 in the calculation as described above. These results indicate that the working gas flowed without an enough extending in the regenerator.

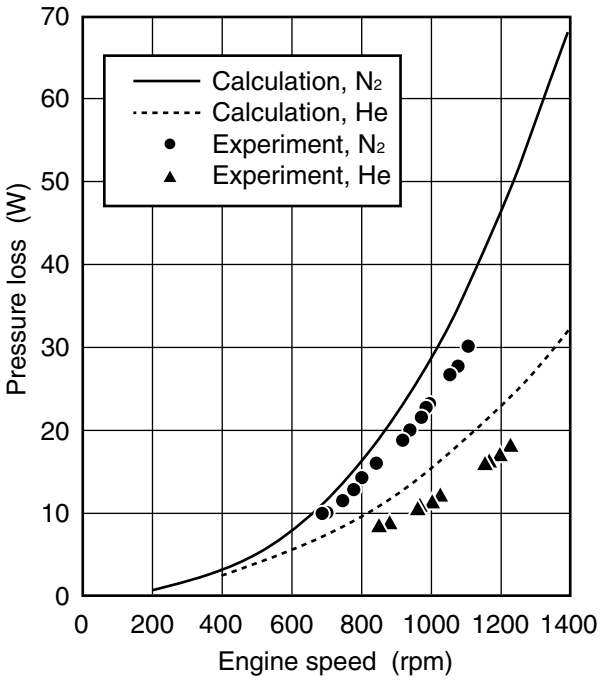

Figure 6 PRESSURE LOSS AS A FUNCTION OF ENGINE SPEED

BUFFER SPACE LOSS

Figure 7 shows the relation between the engine speed and the buffer space loss for both the calculation and the experiment. In this figure, the calculated results of the isothermal model and the adiabatic model were greatly smaller than the experiment results.

On the other hand, the result of the heat transfer model corresponded with the experimental result, when the number of heat transfer unit, N_{tu} was set to 0.1. This value of the unit number doesn't have a basis analytically. We should have more detail discussions about the heat transfer

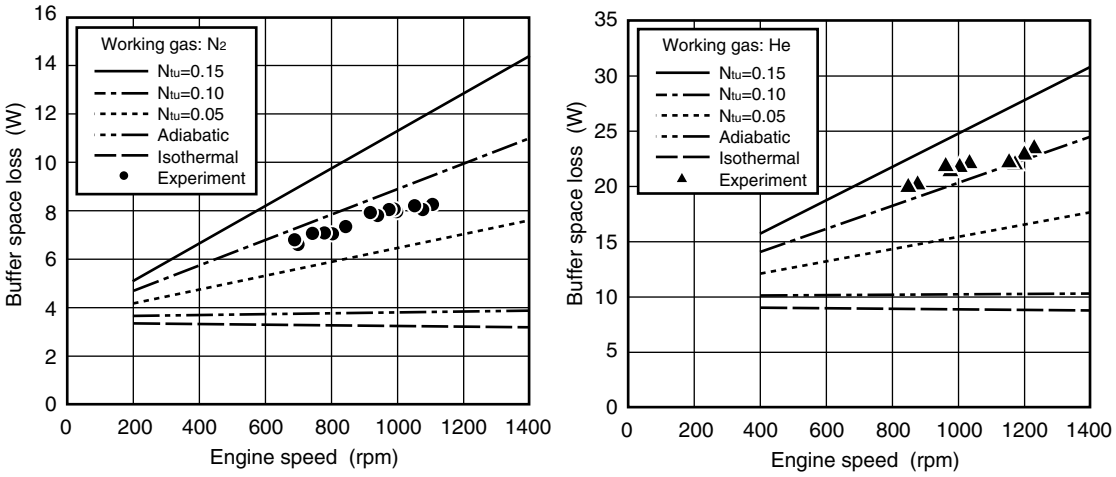

(a) Nitrogen (b) Helium

Figure 7 BUFFER SPACE LOSS AS A FUNCTION OF ENGINE SPEED

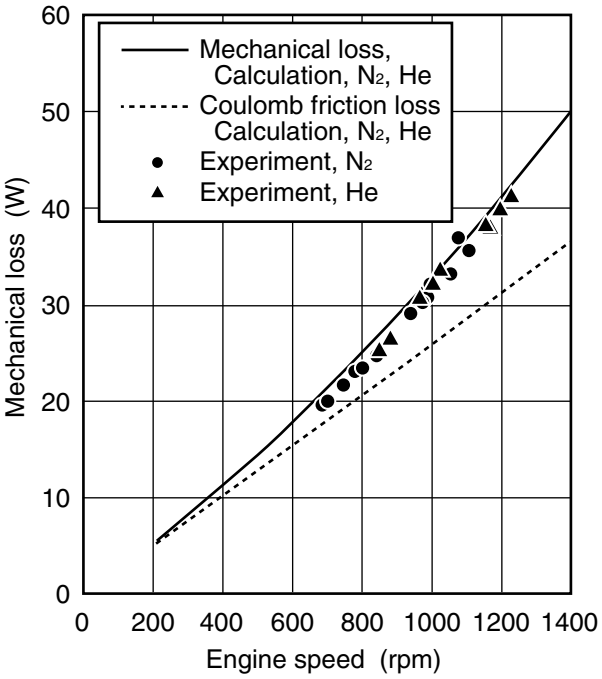

Figure 8 MECHANICAL LOSS AS A FUNCTION OF ENGINE SPEED

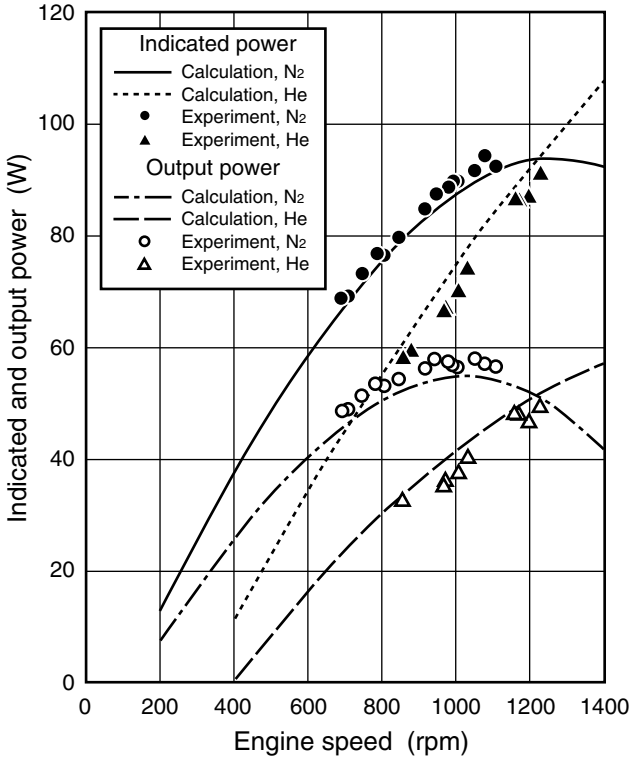

Figure 9 POWER AS A FUNCTION OF ENGINE SPEED

in the buffer space.

The buffer space loss using helium as the working gas was about two times as large as that of nitrogen. It is considered that the effect of the gas leakage appeared strongly.

MECHANICAL LOSS

Figure 8 shows the relation between the engine speed and the mechanical loss. This figure shows that the calculation of the coulomb friction loss has a quadratic increasing to the engine speed. This means that there is few effect of piston inertia forces.

As one can see from this figure, the mechanical loss can be simulated well, when the viscosity friction loss based the experimental result is considered.

INDICATED POWER AND SHAFT POWER

Figure 9 shows the relation between the engine speed and the indicated and output power. This figure shows the calculated results agree with the experimental result well. In this calculation, the heat transfer model with N_{tu}=0.1 was used for the buffer space.

The indicated and output powers with nitrogen are larger than the powers obtained with helium greatly. It is considered that the cause was the large gas leakage from the piston ring and the lip seal mainly.

DISCUSSION BY ANALYSIS MODEL

As described above, it was confirmed that the analysis model can simulate the performance of the prototype engine. The way of improvements of the engine performance are discussed in this chapter.

EFFECT OF GAS LEAKAGE

Figure 10 shows the relation between the equivalent diameter, d_{leak} and the output power at the engine speed, 1000 rpm. Other conditions are the same to above experiments as shown in this figure. This figure shows that the power using helium is higher than that using nitrogen, when the equivalent diameter is smaller than about 0.7 mm. In the case of above experiment, the engine power using nitrogen was higher than that using helium. It is considered that the large gas leakage caused the characteristic of the prototype engine.

EFFECT OF EXPANSION SPACE TEMPERATURE

In the above experiments, the expansion gas temperature was contained to 703 K, because the electric heater had a limit capacity. This temperature is greatly lower than that of a design process, 923 K.

Figure 11 shows the relation between the expansion temperature, T_E and the output power at the engine speed, 1000 rpm. The calculated result shows that the output power reaches the target power, 100 W approximately at the expansion temperature, 923 K.

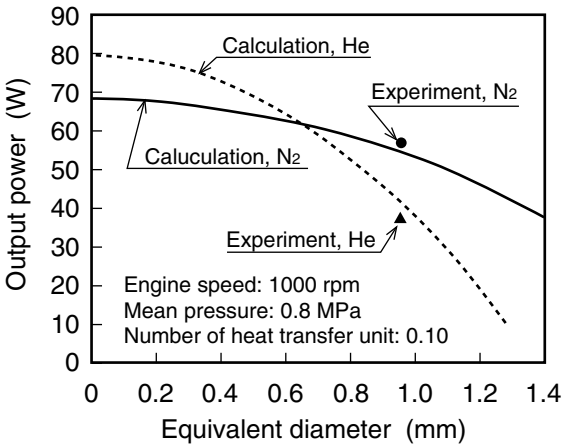

Figure 10 EFFECT OF GAS LEAKAGE

EFFECT OF BUFFER VOLUME

The prototype engine has the small buffer space volume compared with that of a general Stirling engine, because it designed as small as possible. It has a possibility to increase the buffer space loss.

Figure 12 shows the output power and the buffer space loss at 1000 rpm which were obtained with the volume of the current buffer space without any auxiliary buffer tank. When helium is used, especially the power changes with the buffer space volume which influence the buffer space loss.

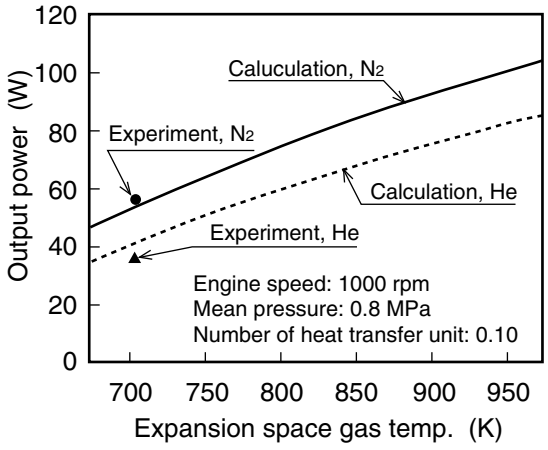

Figure 11 EFFECT OF EXPANSION GAS TEMPERATURE

CONCLUSIONS

The summary of the results is shown below.
(1) The analysis model, which is considered the pressure loss at the regenerator, the gas leakage and the heat transfer in the buffer space was presented. It can simulate the engine performance adequately.
(2) The buffer space loss of the prototype engine is estimated adequately, when it is considered the heat transfer with the number of heat transfer unit, N_{tu}=0.1. The next step of the research will be to discuss the basis of N_{tu}.
(3) It is considered that the working gas flowed without an enough extending in the regenerator in the prototype engine.

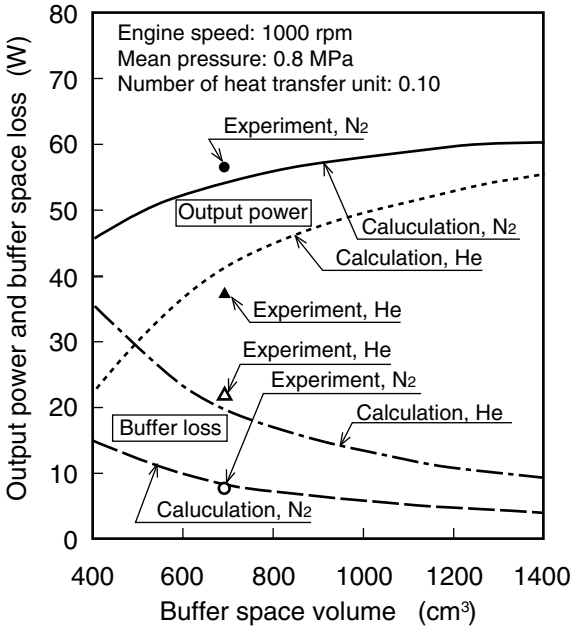

Figure 12 EFFECT OF BUFFER SPACE VOLUME

ACKNOWLEDGEMENT

The prototype engine, Ecoboy-SCM81 is supported by a grant from the Japan Society of Mechanical Engineers. Many people have contributed to the design and development of the prototype engine. The authors thank all members of RC127 committee for their considerable cooperation. We received valuable comments from N. Kagawa.

REFERENCE

1) Kagawa, N., et al., 1995, "Design of Applicative 100 W Stirling Engine," Proceedings, 30th IECEC, p.341.
2) Hirata, K., et al., 1996, "Test Results of Applicative 100 W Stirling Engine, " Proceedings, 31st IECEC, vol.2, p.1259-1264.
3) Kagawa, N., et al., 1995, "Design of A 100 W Stirling Engine," Proceedings, 7th ICSC, Tokyo, JSME, p.211.
4) Tanaka, M., et al., 1989, JSME (in Japanese), Vol.55, No.516, p.2478.
5) Yoshikawa, Y., et al., 1995, "Effect of Entrance Area on the Velocity Distribution in Regenerator Matrix", Preprint of Japan Soc. Mech. Engrs. (in Japanese), No.95-54, p.37-39.
6) Yoshikawa, Y., et al., 1996, "Effect of Entrance and Exit Area on the Velocity Distribution in Regenerator Matrix", Preprint of Japan Soc. Mech. Engrs. (in Japanese), No.96-15, p.499-500.
7) Toyokura, T., et al., 1988, "Hydrodynamics (in Japanese)," p274-280.
8) Kagawa, N., et al., 1989, “Mechanical Analysis and Durability for a 3 kW Stirling Engine", Proc. 24th IECEC, IEEE, p. 2369-2375.